Coupling of Cytochrome and Quinone Turnovers in the Photocycle of Reaction Centers from the Photosynthetic Bacterium *Rhodobacter sphaeroides*

Szabolcs Osváth and Péter Maróti
Department of Biophysics, József Attila University, Szeged H-6722, Hungary

ABSTRACT A minimal kinetic model of the photocycle, including both quinone (Q-6) reduction at the secondary quinone-binding site and (mammalian) cytochrome *c* oxidation at the cytochrome docking site of isolated reaction centers from photosynthetic purple bacteria *Rhodobacter sphaeroides*, was elaborated and tested by cytochrome photooxidation under strong continuous illumination. The typical rate of photochemical excitation by a laser diode at 810 nm was 2.200 s^{-1}, and the rates of stationary turnover of the reaction center (one-half of that of cytochrome photooxidation) were 600 ± 70 s^{-1} at pH 6 and 400 ± 50 s^{-1} at pH 8. The rate of turnover showed strong pH dependence, indicating the contribution of different rate-limiting processes. The kinetic limitation of the photocycle was attributed to the turnover of the cytochrome *c* binding site (pH < 6), light intensity and quinone/quinol exchange (6 < pH < 8), and proton-coupled second electron transfer in the quinone acceptor complex (pH > 8). The analysis of the double-reciprocal plot of the rate of turnover versus light intensity has proved useful in determining the light-independent (maximum) turnover rate of the reaction center (445 ± 50 s^{-1} at pH 7.8).

GLOSSARY

$k_{AB}^{(1)}$	rate constant of $Q_A^- Q_B \rightarrow Q_A Q_B^-$ (first) electron transfer
$k_{AB}^{(2)}$	rate constant of $Q_A^- Q_B^- \rightarrow Q_A (Q_B H)^-$ proton-activated (second) electron transfer
k_C	rate constant of $C^{3+}(RC) + C^{2+} \rightarrow C^{2+}(RC) + C^{3+}$ cytochrome exchange between RC and the pool
k_{cyt}	observed rate of cytochrome turnover, increase in concentration of oxidized cytochrome molecules in unit interval of time: $k_{cyt} = d[C^{3+}]/dt$
k_I	rate constant of $PQ_A \rightarrow P^+ Q_A^-$ photochemical reaction
k_Q	rate constant of $Q_B H_2 \rightarrow Q_B$ quinone exchange
k_{RC}	rate constant of cycling of the RC

INTRODUCTION

Electron and proton transfers are key processes in the generation and interconversion of free energy in living systems. In photosynthetic organisms, the primary electron and proton transfer steps are initiated by the absorption of light and occur in membrane-bound pigment-protein complexes called reaction centers (RCs) (Clayton, 1980). The transfer of reducing equivalents is a cyclic process that requires the presence of exogenous quinones (electron acceptor) and cytochromes (electron donor) in addition to the cofactors of the RC (Feher et al., 1989; Paddock et al., 1994; Okamura and Feher, 1995). The coupled electron and proton transfer across the membrane establishes a proton electrochemical gradient, which drives ATP synthesis catalyzed by ATPase (Crofts and Wraight, 1983; Cramer and Knaff, 1990).

The RC of the non-sulfur purple bacterium *Rhodobacter (Rb.) sphaeroides* is well suited to studies of the photocycle. The crystal structure of the three subunits (L, M, and H) and the cofactors (four bacteriochlorophylls, two bacteriopheophytins, two ubiquinones, and an iron atom) is known with high spatial resolution (Allen et al., 1988; Chang et al., 1986; Ermler et al., 1994; Arnoux et al., 1995), the electron and proton transfer pathways are well characterized and are relatively simple compared to those in higher plants (Crofts and Wraight, 1983; Feher et al., 1989; Maróti, 1993), and a great variety of well-defined mutants are available (Paddock et al., 1988; Takahashi et al., 1989; Tandori et al., 1995).

The source of the light-induced electron flow through the RC is a reduced cytochrome, and the drain is a quinone molecule bound to the RC. The stoichiometry of their reduction/oxidation is different: whereas the cytochrome is oxidized by the release of one electron, the quinone attached to the RC (secondary quinone, Q_B) is reduced by the uptake of two electrons. The function of the electron transfer (the turnover of the RC) should involve continuous turnover of both the cytochromes at the donor side (Fig. 1 *C*) and the quinones at the acceptor side of the RC (Fig. 1 *A*); the oxidized donor and the reduced dihydroquinone (QH_2) are released from the protein and replaced by reduced cytochrome and oxidized quinone from their pools, respectively. The stable states of the mobile (exchangeable) components of the two cycles are connected to the redox states of the cofactors firmly bound to the RC (Fig. 1 *B*). The observed pathway and kinetics of electron transfer through the RC will depend on the coupling of the cytochrome oxidation and quinone reduction cycles.

Received for publication 30 December 1996 and in final form 23 April 1997.

Address reprint requests to Dr. Péter Maróti, Department of Biophysics, József Attila University, Szeged, Egyetem utca 2, H-6722 Hungary. Tel.: 36-62-454-120; Fax: 36-62-454-121; E-mail: pmaroti@physx.u-szeged.hu.

0006-3495/97/08/972/11 $2.00

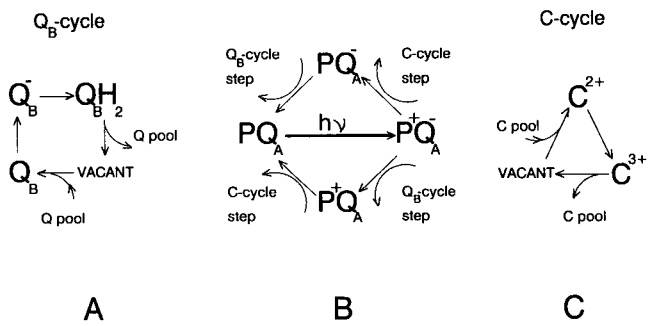

FIGURE 1 Components of the RC photocycle. To the redox states of the firmly bound cofactors of dimer P and primary quinone Q_A (*B*), the different steps of the cytochrome oxidation (*C*) and quinone reduction (*A*) cycles can be coupled at the cytochrome docking site and at the secondary quinone (Q_B) binding site of the RC, respectively. Q_A and the cytochrome are making one-electron chemistry, and the loosely bound Q_B is functioning as a two-electron gate with semireduced (Q_B^-) and fully reduced (QH_2) forms. The cytochrome and quinone molecules at the binding sites are in exchange with those in their pools. The light-induced ($h\nu$) charge separated $P^+Q_A^-$ state can return to the PQ_A state via two pathways, depending on the rates of corresponding steps in the Q_B cycle and the cytochrome cycle. The charge recombination, the transient $Q_A(Q_BH)^-$ state, and the details of proton uptake are omitted.

The fundamental steps and kinetic characteristics of the quinone reduction cycle (McPherson et al., 1990, 1993, 1994; Okamura and Feher, 1992, 1995; Maróti et al., 1995; Graige et al., 1996) and the cytochrome turnover (Overfield and Wraight, 1980; Venturoli et al., 1990; Tiede et al., 1993; Mathis, 1994) upon multiple-flash excitation have been well established in RCs from *Rb. sphaeroides*. Excitation of the RC by a flash results in intraprotein charge separation with a quantum yield of near unity (Fig. 1 *B*) (Wraight and Clayton, 1974). The primary donor (P), a dimer of bacteriochlorophyll, transfers an electron via monomeric bacteriochlorophyll (Arlt et al., 1993) and bacteriopheophytin molecules to the primary quinone acceptor (Q_A) within 200 ps (Feher et al., 1989). Whereas the electron on the bound anionic semiquinone Q_A^- is shared with either Q_B or Q_B^- components of the attached quinone cycle, P^+ can be rereduced if reduced cytochrome is available at the docking site of the RC. Depending on the relative rates of the reactions, either P^+Q_A or PQ_A^- redox states of the RC will be transiently formed before all charges are transported out of the RC.

The photooxidation of cytochrome (cytochrome c_2 in native membrane or added mammalian cytochrome *c* in isolated RC) after single-flash excitation showed complex kinetics (Overfield and Wraight, 1980; Venturoli et al., 1990; Tiede et al., 1993; Mathis, 1994). The fast monomolecular process had a rate constant of $\sim 1 \times 10^6\ s^{-1}$ and was attributed to cytochromes already bound to the RC at the moment of the flash. It was followed by a slower collisional reaction between the cytochrome and the RC, with an observed bimolecular rate constant of $\sim 1 \times 10^9\ M^{-1}\ s^{-1}$. For the cytochrome exchange rate, very rough estimates could be given from double-flash experiments (Venturoli et al., 1990).

After the first electron transfer from Q_A^- to Q_B with a pH-dependent rate constant of $k_{AB}^{(1)} \approx (100\ \mu s)^{-1}$ at near-neutral pH (Vermeglio and Clayton, 1977; Wraight, 1979; Kleinfeld et al., 1984), a second flash excitation of the RC results in the photochemically inactive $Q_A^-Q_B^-$ state (Wraight, 1981). The transfer of the second electron to the secondary quinone acceptor is reversibly coupled to the uptake of the first proton and results in the $Q_A(Q_BH)^-$ state (Kleinfeld et al., 1985; Graige et al., 1996). The rate constant of the first proton-coupled second electron transfer, $k_{AB}^{(2)}$, is also pH dependent (Paddock et al., 1994). The uptake of the second proton finally forms dihydroquinone (Q_BH_2) (Wraight, 1979; McPherson et al., 1994; Takahashi and Wraight, 1996; Graige et al., 1996). In some protonation mutants (mainly those mutated Glu at position L212), the second proton transfer to the $Q_A(Q_BH)^-$ state becomes very slow (Takahashi and Wraight, 1992, 1996; Paddock et al., 1994; Maróti et al., 1994; Okamura and Feher, 1995), and a third flash excitation leads to the formation of the $Q_A^-(Q_BH)^-$ state, which transforms to $PQ_A^-Q_BH_2$ simultaneously with the slow kinetics of the second proton uptake. In wild-type RCs, however, the accumulation of the $Q_A^-(Q_BH)^-$ state in the quinone reduction cycle is not significant; therefore it is not included in Fig. 1.

The generally accepted working model for the photocycle of isolated RCs is based primarily on multiple-flash excitation experiments and, if the finite rates of exchanges of quinone/quinol and reduced/oxidized cytochromes are taken into account, they are treated in a qualitative manner only (Paddock et al., 1988, 1994). An estimate larger than 500 s^{-1} for the rate of cytochrome photooxidation is generally accepted (Okamura and Feher, 1995). The RCs of photosynthetic organisms, however, are exposed to continuous illumination under natural conditions, where both the quinones and the cytochromes should turn over continuously and the quantitative interpretation is highly complicated by the kinetic interference of the electron transfer steps for "opening" the RC (Fig. 1; Venturoli et al., 1990; Shinkarev, 1990).

Here the pH dependence of the cycling rate, the rate-limiting steps, and their contribution to the observed turnover, with special regard to the donor and acceptor sides, will be studied. A minimal kinetic model for the analysis of the kinetics of the photocycle after the rectangular shape (unit step) of excitation will be presented. It will be shown that the analysis of the turnover of the RC offers direct determination of the exchange rates of quinone/quinol and cyt c^{2+}/cyt c^{3+} at the acceptor and donor sides of the RC, respectively.

MATERIALS AND METHODS

Rhodobacter sphaeroides cells were disrupted by French press, and chromatophores were prepared as described earlier (Maróti and Wraight, 1988). The RCs were solubilized in 0.55% lauryl dimethylamine-*N*-oxide (LDAO) and purified by ammonium sulfate precipitation and repeated ion-exchange chromatography on DEAE-Sephacel until the ratio between

the absorbance at 280 nm and 800 nm (OD(280 nm)/OD(800 nm)), reflecting purity, dropped below 1.30. RCs were depleted of secondary quinones as described (Okamura et al., 1975). The secondary quinone activity was reconstituted with UQ_6 (Sigma), added in excess from a 10 mM stock solubilized in ethanol. The concentration of photochemically active RCs was determined from flash-induced absorption change at 430 nm or 865 nm (Maróti and Wraight, 1988).

Horse heart cytochrome *c* (Sigma) was used as external donor to P^+, and its oxidation was monitored optically at 550 nm. The amount of cyt c^{2+} oxidized by RCs was determined with the difference extinction coefficient $\epsilon_{red} - \epsilon_{ox} = 21.1 \pm 0.4\ mM^{-1}\ cm^{-1}$ (Van Gelder and Slater, 1962). Cytochrome *c* was reduced before use. The solution of 4 mM cytochrome *c* and 40 mM sodium ascorbate was loaded onto a PD-10 column containing Sephadex G-25M gel (Pharmacia). The reduced ascorbate-free cytochrome *c* was collected and the free sodium ascorbate was retained by the column. The free sodium ascorbate would reduce part of the exogenous quinone pool, and thus the photooxidized cytochrome *c* would artificially decrease the observed rate of RC turnover. The ionic strength of the solution was kept low to ensure fast cytochrome photooxidation. The assay solution was 0.03% Triton X-100/25 μM ubiquinone (Q-6)/100 μM reduced cyt *c*/2 mM buffer (succinate, MES (4-morpholineethanesulfonic acid), PIPES (1,4-piperazinediethanesulfonic acid), Tris (2-amino-2-hydroxymethylpropane-1,3-diol), or CHES (2-(*N*-cyclohexylamino)ethanesulfonic acid), depending on the pH) and ~1 μM RC.

The kinetic steps were followed by optical spectroscopy performed on a kinetic spectrophotometer of local design (Maróti and Wraight, 1988; Osváth et al., 1996). Actinic illumination was provided either by Xe flash (EG&G FX-200) or by a laser diode (Laser Diode; type LCW-100, emission wavelength 810 nm, power 500 mW). Because of the very short rise and fall times (100 ns) of the laser diode, the pulsed illumination by the laser diode could be considered a "rectangular shape of excitation" in our time frame. The light from the laser diode was homogenized and focused on a 3 × 3 mm^2 cross-sectional area of the measuring quartz cuvette. Different light intensities were achieved by attenuation of the exciting beam with neutral filters. An IBM-compatible personal computer was used for model calculations and data analysis.

All measurements were made at room temperature (23°C).

RESULTS

The different steps in the photocycle can be followed by direct optical detection of formation and disappearance of semiquinones in the quinone reduction cycle (Fig. 1 *A*) or oxidized cytochrome *c* in the cytochrome cycle (Fig. 1 *C*). Unfortunately, the absorption coefficients of the various semiquinone states and their differences are small (Kleinfeld et al., 1985; McPherson et al., 1994), but the measurement of cytochrome photooxidation is an excellent method of tracking the steps of the photocycle (Okamura and Feher, 1995). The RC undergoes charge separation and subsequent cytochrome oxidation in any of the open (PQ_A, PQ_AQ_B, $PQ_AQ_B^-$, and $PQ_AQ_BH_2$) states of the RC after onset of the illumination. The kinetics of cytochrome photooxidation under the rectangular shape of excitation from the laser diode may consist of three distinct phases (Fig. 2). The constant rate of the cytochrome turnover, k_{cyt} (stationary phase), is achieved after a short transient period after the onset of the illumination (initial phase), and the observed rate of the stationary phase decreases gradually after prolonged illumination (saturation phase). Experiments were carried out to understand the origin and characteristics of the different phases.

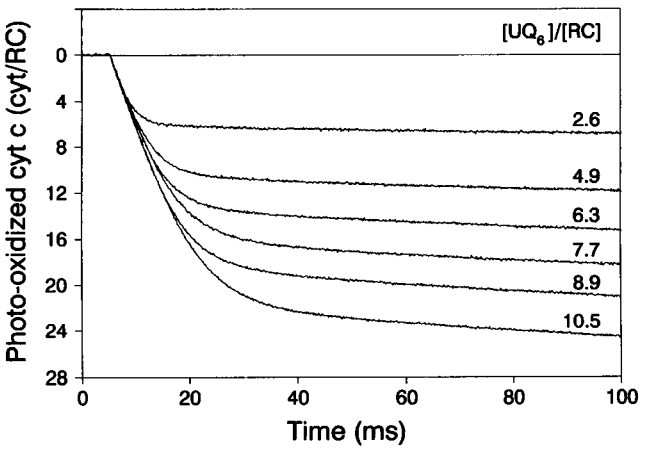

FIGURE 2 Kinetics of cytochrome *c* photooxidation in RCs of *Rb. sphaeroides* in the presence of different quinone (UQ_6) pool sizes and excess cytochrome *c* under intense continuous laser diode excitation at 810 nm. The transmission changes detected at 550 nm were converted to absorption changes to determine the quantity of oxidized cytochrome *c*. The amounts of quinone externally added to Q_B-less RC and photooxidized cytochrome *c* are referred to the concentration of the RC. Conditions: 0.9 μM RC, 0.03% TX-100, 200 μM cyt *c*, 5 mM Tris, pH 7.5, and $k_l = 2.2 \times 10^3\ s^{-1}$.

Saturation phase

The observed rate of the cytochrome turnover depends on the pool sizes of quinones and cytochromes and decreases if any of the pools approaches exhaustion. It is demonstrated in two separate titration experiments in which one of the pools is significantly larger than the other.

In Fig. 2, the kinetics of cytochrome photooxidation is shown in samples of a large cytochrome pool and a partly filled Q_B binding site incubated with different quinone concentrations and excited by the same light intensity. Similar experiments were carried out earlier with a restricted range of quinone concentration (Okamura et al., 1982). The slopes of the titration curves were initially identical, but flattened later when the number of cytochrome turnovers approached the size of the quinone pool. The transition period was short. A very slow, gradual increase in cytochrome oxidation could be observed, even in the case in which the quinone pool was exhausted. The rate was determined from the slope of the cytochrome signal between 0.4 s and 0.5 s (not shown in Fig. 2), and $k_{OX} = 1.9\ s^{-1}$ was obtained. This rate is several orders of magnitude smaller than any of the reactions considered in the photocycle. We attributed this effect to a slow reoxidation of the accumulated dihydroquinone by an unidentified redox agent in the solution. In this way, the reoxidized QH_2 is able to turn over additional RCs (and cytochromes). In the case of water-soluble UQ_0, the oxidized cytochrome itself can reoxidize the reduced forms of the quinone, but the rates are much smaller than those of any competitive reactions in the photocycle (Van Rotterdam et al., 1995). For the hydrophobic UQ_6 embedded in the detergent micelle, the redox interac-

tion of oxidized cytochrome and reduced quinones can have a negligible effect on the fast kinetics of the photocycle.

The results of an alternative study with a large quinone pool and an easily exhaustible reduced cytochrome pool can be seen in Fig. 3. In contrast to the quinone titration, the initial slopes are not constant, but increase with increasing external cytochrome *c* concentrations. The saturation level of the cytochrome turnover is in good agreement with the size of the cytochrome *c* pool.

Stationary phase

The kinetics of cytochrome turnovers were recorded during different light intensities of rectangular shape in the presence of excess quinones and cytochromes (Fig. 4). The intensity of excitation is expressed in terms of k_I, the rate constant of the photochemical reaction $PQ_A \rightarrow P^+Q_A^-$ (Fig. 1 *B*). It was determined from the exponential fitting of the rise of absorbance at 865 nm induced by the onset of the laser diode in the absence of cytochrome *c*. The observed rate of cytochrome photooxidation depends clearly on light intensity and starts to decrease after 8–10 turnovers because of saturation events studied above. The rates of stationary cytochrome turnover were derived from the section between 5 and 7 cyt/RC, where the initial (see below) and saturation phases have minor effects. The reciprocity between the stationary turnover time and the light intensity can be well demonstrated by a double-reciprocal plot of the rates (k_{cyt}^{-1} versus k_I^{-1}; Maróti et al., 1995; Fig. 5). At low light intensities, the measured values can be fitted by a straight line with good approximation, and the intercept of the vertical axis (linear extrapolation to $1/k_I = 0$) represents the maximum (light-saturated) cycling rate of the RC. Slight deviation from the linearity can be observed at high light intensities, which calls attention to the importance of a proper model to the determination of the light-saturated turnover rate.

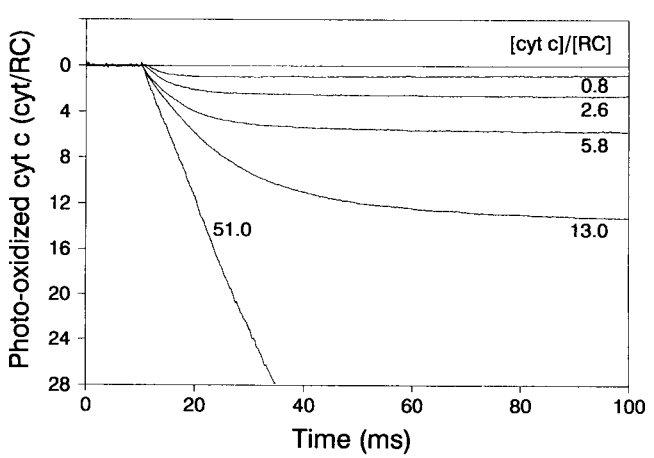

FIGURE 3 Kinetics of cytochrome *c* photooxidation at large quinone pool (50 μM UQ_6) and variable cytochrome *c* pool size under strong laser diode illumination. The conditions are otherwise the same as in Fig. 2.

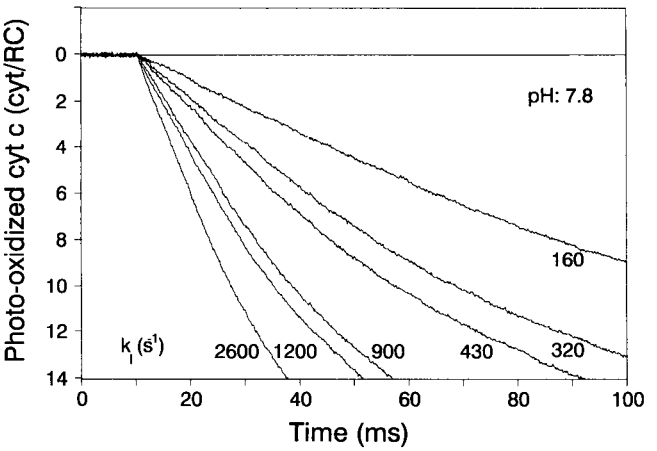

FIGURE 4 Light intensity dependence of the kinetics of cytochrome *c* photooxidation induced by the rectangular shape of illumination in RCs of *Rb. sphaeroides*. The different light intensities were adjusted by neutral density filters and were expressed as photochemical rate constants (k_I) indicated at the curves. A light intensity of 5 W cm^{-2} from a laser diode (810 nm) corresponded to a photochemical rate constant of $k_I = 2.6 \times 10^3$ s^{-1}. Conditions: 1.5 μM RC, 0.03% TX-100, 25 μM QU_6, 100 μM cyt *c*, and 5 mM Tris at pH 7.8.

Initial phase

The kinetics of cytochrome photooxidation deviates from linearity, not only close to the exhaustion of any of the pools, but also at the onset of illumination. This can be shown on the kinetics measured in the alkaline pH range (Fig. 6). The turnover of the first ~1.5 cytochromes at pH 9.5 is very fast (as fast as the stationary turnover of the RC at pH 7.1), but the subsequent photooxidation is significantly slower. Similar biphasic turnover cannot be observed in the acidic and near-neutral pH ranges. The position of the break point that determines how many cytochromes can turn

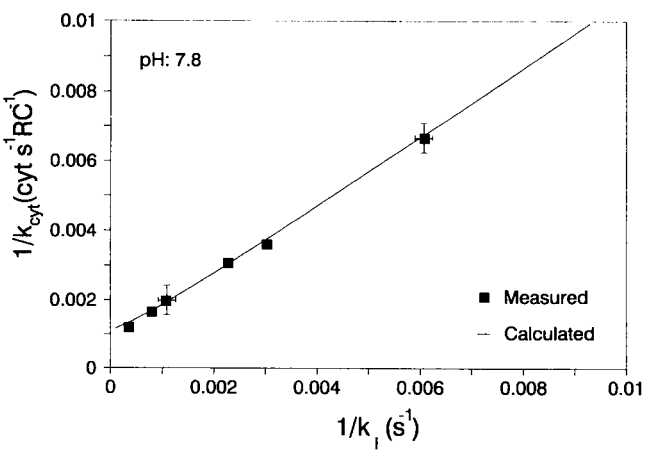

FIGURE 5 Determination of light-independent (maximum) turnover rate of RCs of *Rb. sphaeroides* by a double-reciprocal plot of the turnover rate of RC (k_{RC}) and the photochemical rate constant (k_I). The data (■) were derived from cytochrome turnovers shown in Fig. 4. The fit (——) was calculated from Eq. 3 with $k_{AB}^{(1)} = 5.5 \times 10^3$ s^{-1}, $k_{AB}^{(2)} = 10^3$ s^{-1}, $k_C = 2 \times 10^3$ s^{-1}, and $k_Q = 950$ s^{-1}.

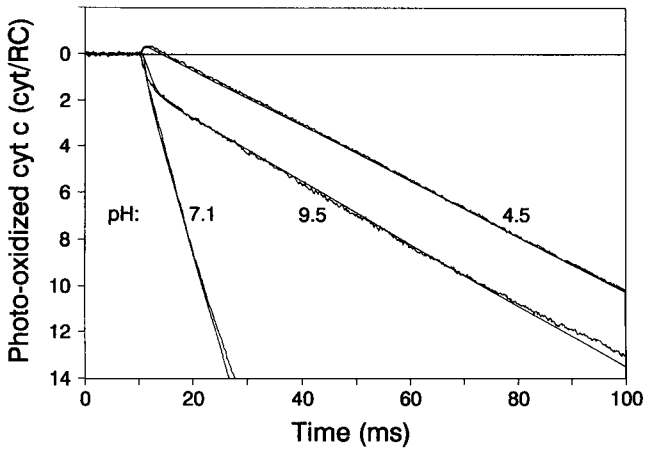

FIGURE 6 The pH dependence of the kinetics of cytochrome *c* photooxidation in RCs of *Rb. sphaeroides* under a rectangular shape of excitation. The best fits to the traces (——) were obtained by $k_C = 145\ s^{-1}$ and $k_Q = 2.000\ s^{-1}$ at pH 4.5, $k_C = 4.000\ s^{-1}$ and $k_Q = 950\ s^{-1}$ at pH 7.1, and $k_C = 1.100\ s^{-1}$ and $k_Q = 1.000\ s^{-1}$ at pH 9.5. By fitting the initial phase at pH 4.5, 12 $mM^{-1}\ cm^{-1}$ was taken for the absorption coefficient of P/P^+ at 550 nm (Maróti et al., 1985). Conditions: $k_I = 2.2 \times 10^3\ s^{-1}$, 1.2 μM RC, 0.03% TX-100, 25 μM UQ_6, 100 μM cyt *c*, and 5 mM buffer (succinate, Tris, or CHES), depending on pH.

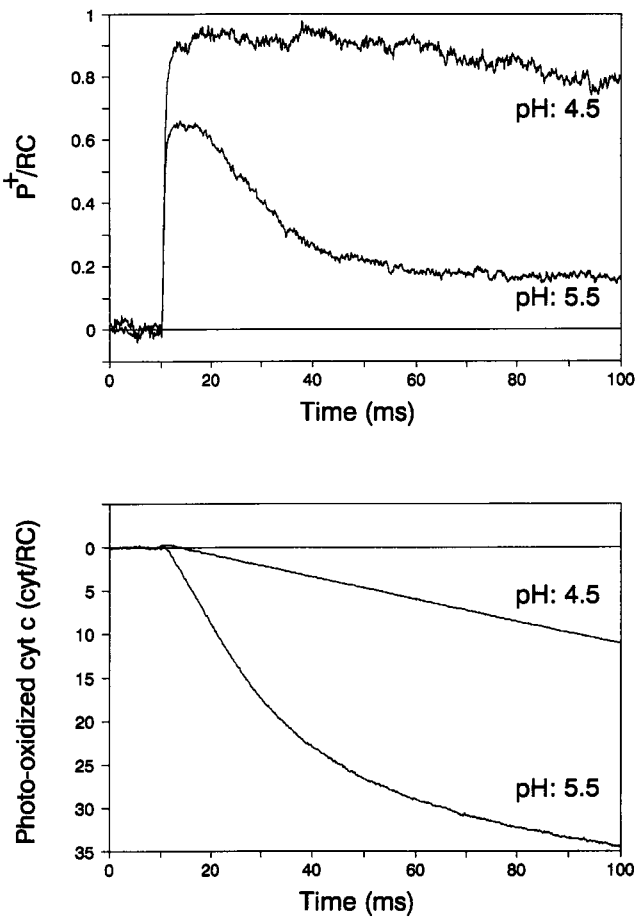

FIGURE 7 Kinetic comparison of cytochrome *c* photooxidation (550 nm) and P^+ accumulation (865 nm) under continuous laser diode excitation (810 nm) in the initial and stationary phases and close to the saturation phase of the turnover at pH 4.5 and 5.5. Conditions: $k_I = 2.2 \times 10^3\ s^{-1}$, 1.1 μM RC, 0.03% TX-100, 25 μM UQ_6, 100 μM cyt *c*, and 5 mM buffer (MES at pH 5.5 and succinate at pH 4.5).

over quickly correlates inversely with the electron equilibrium constant of the acceptor quinone complex, K_{AB}. At pH 9.5, K_{AB} is significantly less than that measured at neutral and acidic pH values (Kleinfeld et al., 1984), and the break point could be well resolved.

The other side of the pH scale also shows an interesting property of the initial phase of the kinetics. A small increase is followed by a linear absorption change at acidic pH (Fig. 6). A delay of ~5 ms can be calculated between the onset of illumination and the inception of the stationary phase at pH 4.5. The lag phase, however, does not originate from the cytochrome turnover, but from the formation of oxidized dimer, P^+. The P/P^+ redox change makes some contribution to the observed absorption change due to cytochrome oxidation at 550 nm (Maróti et al., 1985).

Cytochrome *c* donation at low pH

Simultaneously with the cytochrome photooxidation, the kinetics of P^+ was also monitored by the absorption change at 865 nm, where the contribution of cytochrome is negligible (Fig. 7). A significant accumulation of oxidized dimer was observed in the acidic pH range during the stationary phase of the cytochrome photooxidation, which indicated a dramatic decrease in the rate of cytochrome oxidation at pH < 6. The concentration of P^+, however, started to decrease as soon as the quinone pool approached exhaustion, because the deceleration of quinone exchange made it possible for the cytochrome to reduce more P^+. Thus, without a significant change in the cytochrome turnover, the loss of accumulated P^+ forecasted the decline in the cycling rate of the RC. The drop in P^+ concentration proved to be more sensitive to the deceleration of the turnover of the RC than the decrease in cytochrome photooxidation.

The cytochrome/RC complex was also studied by flash excitation at low pH. The P^+ re-reduction by cytochrome *c* after a single saturating flash was two to three orders of magnitude slower at low pH than at neutral pH, and the kinetics was very sensitive to the concentration of cytochrome *c* (Fig. 8). These experiments reveal a mechanism of reaction similar to that which has been substantially discussed in the literature for higher pH (Overfield and Wraight, 1980; Venturoli et al., 1990, 1993; Tiede and Chang, 1988; Tiede et al., 1993; Mathis, 1994). At acidic pH, however, the bimolecular (collisional) process dominated over the monomolecular kinetics, even at high cytochrome *c* concentration (200 μM). A second-order rate constant of $4.4 \times 10^6\ M^{-1}\ s^{-1}$ was measured at pH 5.0. The lack of significant contribution of the first-order electron transfer, which is characteristic of the bound cytochrome/RC complex, indicated that the rate constant of the docking of the cytochrome *c* to the RC decreased dramatically at acidic pH.

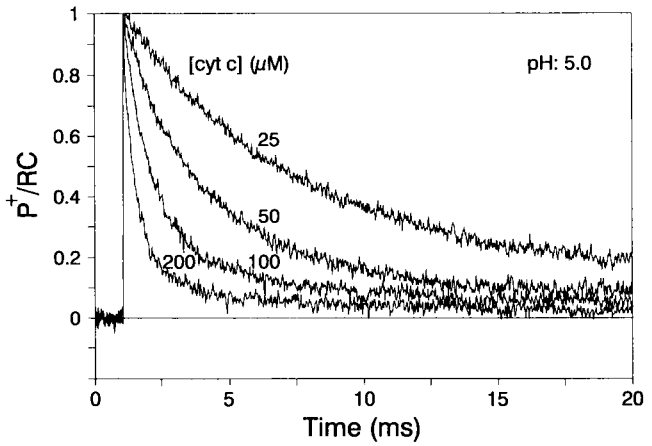

FIGURE 8 Kinetics of P^+ re-reduction by cytochrome *c* in RCs of *Rb. sphaeroides* at low pH. The dimer was oxidized by single saturating flash, and the traces were tracked by changes in absorbance at 865 nm. The concentration of externally added cytochrome *c* is indicated at the traces. Conditions: 1.2 μM RC, 0.03% TX-100, 25 μM QU_6, and 5 mM succinate.

pH dependence of rates and turnovers

Because of the significantly decelerated cytochrome turnover at low pH, significant accumulation of the P^+ state was observed during the stationary phase of the cytochrome photooxidation (Fig. 7). The pH dependence of stationary P^+ accumulation showed a steep increase below pH 6 and a small peak around pH 7.5 (Fig. 9). From the fraction of RC in the P^+ state during stationary turnover, the rate constant of cytochrome exchange can be deduced directly:

$$k_C = 2 \cdot \frac{[RC]}{[P^+]} \cdot k_{RC} \qquad (1)$$

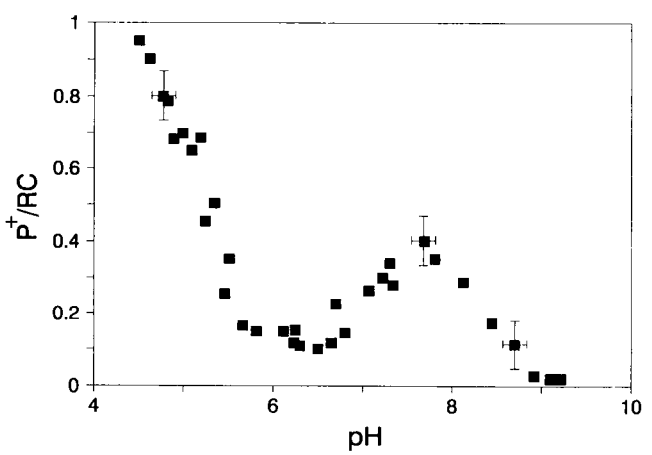

FIGURE 9 The pH dependence of the P^+ accumulation in the stationary phase of the cytochrome *c* photooxidation of RC from *Rb. sphaeroides* (see Fig. 7). The standard deviations of the means are indicated by error bars. Conditions: $k_I = 2.2 \times 10^3\ s^{-1}$, 1.1 μM RC, 0.03% TX-100, 25 μM UQ_6, 100 μM cyt *c*, 5 mM succinate, MES, PIPES, Tris, or CHES, depending on pH.

Here k_{RC} is the rate constant of stationary cycling of the RC, which can be determined from the observed rate of cytochrome photooxidation:

$$k_{RC} = \frac{1}{2} \cdot \frac{(d[C^{3+}])/dt}{[RC]} \qquad (2)$$

This is in accordance with the two-electron gate function of the secondary quinone, as two cytochrome molecules must be oxidized during one turnover of the RC.

In Fig. 10, the rate constants of cytochrome exchange (k_C) calculated from Eq. 1, using data of Fig. 9 and RC turnover (k_{RC}) determined from Eq. 2, are plotted as a function of pH, together with the rates of photochemical reaction (k_I) and electron transfer ($k_{AB}^{(1)}$, $k_{AB}^{(2)}$) taken from the literature (Kleinfeld et al., 1984, 1985; Paddock et al., 1994). In the case of strong excitation ($k_I = 2.2 \times 10^3\ s^{-1}$), the rate constant of the stationary photocycle depends on pH: it has a broad maximum ($k_{RC} = 600\ s^{-1}$) around pH 6 and a somewhat smaller and narrower plateau ($k_{RC} = 400\ s^{-1}$) at pH 8, and decreases toward the rims of the pH scale. The slope of decrease is larger in the acidic (pH < 6) than in the alkaline (pH > 8.5) pH range.

DISCUSSION

Not all of the observed characteristics of the photocycle of bacterial RC can be interpreted in terms of a simple figure like that in Okamura and Feher (1992), where the cytochrome and quinone exchanges were not explicitly included in the model. Here, in addition to a qualitative description, we try to offer a quantitative explanation for the function of the photocycle without using a highly sophisticated model.

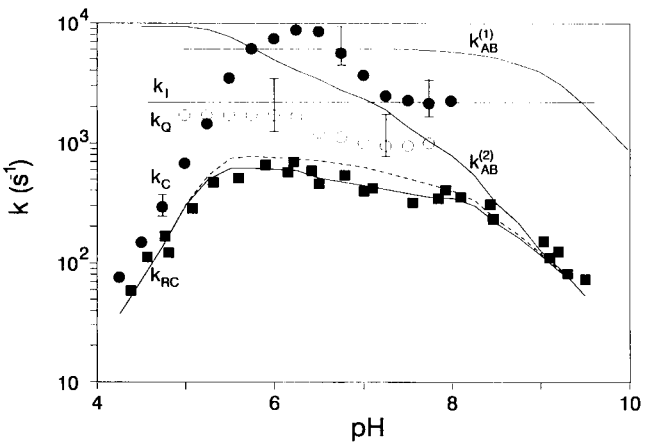

FIGURE 10 The pH dependence of rates of electron transfer ($k_{AB}^{(1)}$ and $k_{AB}^{(2)}$), quinone (k_Q), and cytochrome (k_C) exchange and RC turnover (k_{RC}) in RCs of *Rb. sphaeroides*, together with the (pH independent) photochemical rate constant (k_I). The rate of cytochrome exchange (●) was derived from data in Fig. 9, using Eq. 1. The rate of quinone exchange (k_Q) was obtained from the best fit of the model (○) to the measured cycling rate of the RC (■). The fit with very large quinone exchange rate ($k_Q \rightarrow \infty$) is also demonstrated (– – –) and $k_{AB}^{(1)}$ and $k_{AB}^{(2)}$ were taken from Kleinfeld et al. (1984) and Paddock et al. (1994), respectively.

The discussion will focus on the elaboration and consequences of a minimal kinetic model and the rate-limiting processes of the turnover under photostationary conditions.

Kinetic model of the photocycle

As presented in Fig. 1, the electron transfer within the RC is combined with quinone and cytochrome binding and unbinding processes during the photocycle. The cytochrome docking site can exist in three different states: vacant, or filled with reduced (C^{2+}) or oxidized (C^{3+}) cytochrome *c* (Fig. 1 *C*). Similarly, the secondary quinone site can form four different states, including vacancy and binding of oxidized (Q_B), semireduced (Q_B^-) or fully reduced (Q_BH_2) quinones (Fig. 1 *A*). Their binding affinities are different: the semiquinone binds $\sim 10^5$ times more tightly than the (oxidized) quinone, which binds ~ 10 times more strongly than the dihydroquinone (Wraight and Shopes, 1989; McPherson et al., 1990; Shinkarev and Wraight, 1993). As the semireduced quinone at the Q_B binding site is very stable, the turnover of the quinone reduction cycle depends on the availability of quinone and dihydroquinone and their competition to the Q_B binding site of the RC (Taoka et al., 1983). As the RC-bound cofactors P and Q_A can have four different redox states (Fig. 1 *B*), altogether, $3 \times 4 \times 4 = 48$ possible states of the RC can be distinguished in general case. This number, however, can be significantly reduced under the present conditions. From the point of view of the photocycle, the vacant binding sites and those occupied by oxidized cytochrome or dihydroquinone can be considered identical: vacant $\equiv C^{3+}$ and vacant $\equiv Q_BH_2$, as all behave similarly (i.e., they block the turnover of the RC). The number of the remaining ($2 \times 3 \times 4 = 24$) possible states can be further decreased by taking into account the reasonable rates in the photocycle: if the reduced cytochrome *c* is already bound to the docking site of the RC, then the electron transfer to the oxidized dimer is very fast (Overfield and Wraight, 1980; Tiede et al., 1993; Venturoli et al., 1993; Mathis, 1994). Thus the six transient states including $C^{2+}P^+$ could be omitted, and only the remaining 18 stable forms of the RC should be involved in the photocycle (Fig. 11).

The connections between states include single steps of either light reaction (k_I), electron transfer ($k_{AB}^{(1)}$ and $k_{AB}^{(2)}$ in concert with the first proton uptake), or exchange of quinone (k_Q) or cytochrome *c* (k_C). The "closed" states of the RC ($P^+Q_A^-$, PQ_A^-, and P^+Q_A) are photochemically inactive. In our scheme, the exchange of quinone includes the uptake of the second proton (the final step in formation of Q_BH_2), the release of dihydroquinone, and binding of quinone to the Q_B site.

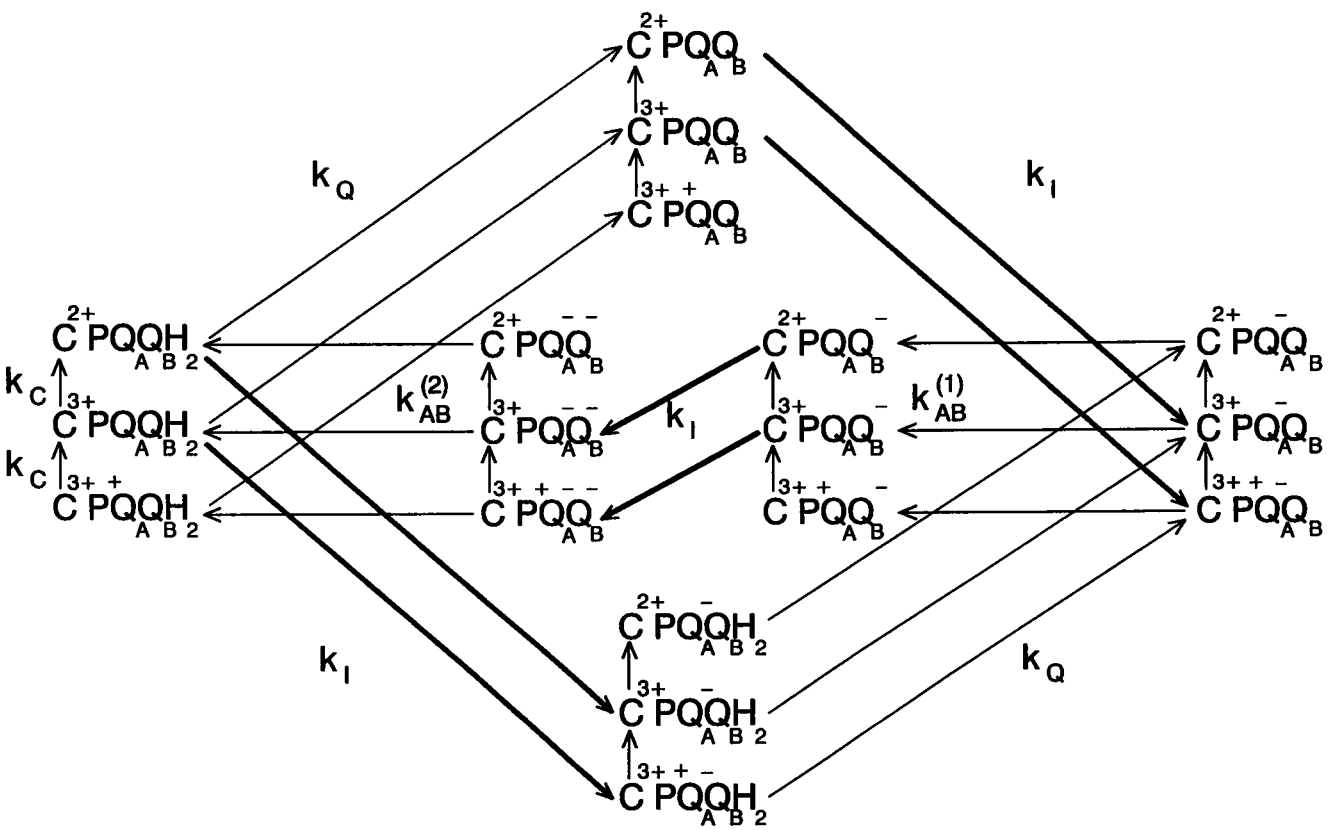

FIGURE 11 Scheme of the photocycle model used to calculate the turnover rate of the RCs under different conditions (Figs. 5, 6, and 10). The model was adapted to our conditions from the more general scheme presented in Fig. 1. For details see text.

Temporal changes of the concentrations of the different states relative to that of the RC can be expressed by solution of the following set of differential equations expressed in matrix form:

$$\frac{d}{dt}[\mathbf{X}] = \mathbf{K} \cdot [\mathbf{X}] \tag{3}$$

where **X** is the column vector of the states and **K** is a 18 × 18 matrix constructed from the rate constants, as seen in Table 1. As cytochrome oxidation can arise from direct photochemical excitation of $C^{2+}PQ_A\cup$ states and from cytochrome exchange and subsequent re-reduction of P^+ in the $C^{3+}P^+\cup\cup$ states of the RC, the observed rate of cytochrome turnover can be calculated from

$$\frac{d}{dt}[C^{3+}] = (\sum[C^{2+}PQ_A\ \cup\ ]) \cdot k_I + (\sum[C^{3+}P^+\ \cup\ \cup\ ]) \cdot k_C \tag{4}$$

The summations should be extended to all Q_B forms of the $C^{2+}PQ_A\cup$ and all possible Q_A and Q_B forms of the $C^{3+}P^+\cup\cup$ states of the RC that include three and six terms on the right-hand side of Eq. 4, respectively. In cases of large quinone and cytochrome *c* pools, the rates in matrix **K** are constant, and the initial and stationary phases of the cytochrome turnovers can be given, even in analytical forms. If any of the pools becomes significantly exhausted, the k_Q and/or k_C exchange rates (as quasi-monomolecular rate constants; McComb et al., 1990) will drop and become time dependent.

The analytical expressions for stationary turnover (even in reasonable special cases) are too complicated; therefore the results were obtained by numerical integration of Eq. 3 (Figs. 5, 6, and 10). The experimental and calculated turnover rates showed good agreement (Fig. 10), and the calculated kinetics fitted to the measured curves with rate constants listed in the figure legends and plotted in Fig. 10.

There are at least two reasons why an initial phase appears in the cytochrome photooxidation kinetics. The dark period before onset of the continuous excitation sets quinone and cytochrome to the binding sites according to their equilibrium binding constants. Thus the initial rate of turnover reflects reactions with already bound mobile carriers, which is not the case in stationary turnover of the RC, where the exchange processes should also be considered. Furthermore, the initial phase subsequently sets the different electron transfer reactions into motion, whereas their combination operates in stationary mode.

The model can account for the separation of the initial and stationary phases of the cytochrome photooxidation at alkaline pH and for the ~5-ms delay at low pH (Fig. 6). These effects can be rationalized by pH-dependent sharing of the first electron in the acceptor quinone complex and the contribution of P/P^+ redox change at the monitoring wavelength, respectively. Because of the bound quinone and cytochrome of the binding sites at the onset of the illumination, the first electron arrives at the acceptor complex with the rate of light excitation. It is shared between Q_A and Q_B according to the electron equilibrium constant, which determines the fraction of $Q_AQ_B^-$ state capable of additional fast reduction. The further (stationary) reduction of the

Table 1 Matrix of rate constants, K and vector of states, X

$$\mathbf{K} = \begin{bmatrix}
-k_I & k_C & 0 & 0 & 0 & 0 & k_Q & 0 & 0 & 0 & 0 & 0 & 0 & 0 & 0 & 0 & 0 & 0 \\
0 & -(k_I+k_C) & k_C & 0 & 0 & 0 & 0 & k_Q & 0 & 0 & 0 & 0 & 0 & 0 & 0 & 0 & 0 & 0 \\
0 & 0 & -k_C & 0 & 0 & 0 & 0 & 0 & k_Q & 0 & 0 & 0 & 0 & 0 & 0 & 0 & 0 & 0 \\
0 & 0 & 0 & -k_{AB}^{(1)} & k_C & 0 & 0 & 0 & 0 & k_Q & 0 & 0 & 0 & 0 & 0 & 0 & 0 & 0 \\
k_I & 0 & 0 & 0 & -(k_C+k_{AB}^{(1)}) & k_C & 0 & 0 & 0 & 0 & k_Q & 0 & 0 & 0 & 0 & 0 & 0 & 0 \\
0 & k_I & 0 & 0 & 0 & -(k_C+k_{AB}^{(1)}) & 0 & 0 & 0 & 0 & 0 & k_Q & 0 & 0 & 0 & 0 & 0 & 0 \\
0 & 0 & 0 & 0 & 0 & 0 & -(k_Q+k_I) & k_C & 0 & 0 & 0 & 0 & 0 & 0 & 0 & k_{AB}^{(2)} & 0 & 0 \\
0 & 0 & 0 & 0 & 0 & 0 & 0 & -(k_C+k_Q+k_I) & k_C & 0 & 0 & 0 & 0 & 0 & 0 & 0 & k_{AB}^{(2)} & 0 \\
0 & 0 & 0 & 0 & 0 & 0 & 0 & 0 & -(k_C+k_Q) & 0 & 0 & 0 & 0 & 0 & 0 & 0 & 0 & k_{AB}^{(2)} \\
0 & 0 & 0 & 0 & 0 & 0 & 0 & 0 & 0 & -k_Q & k_C & 0 & 0 & 0 & 0 & 0 & 0 & 0 \\
0 & 0 & 0 & 0 & 0 & 0 & k_I & 0 & 0 & 0 & -(k_C+k_Q) & k_C & 0 & 0 & 0 & 0 & 0 & 0 \\
0 & 0 & 0 & 0 & 0 & 0 & 0 & k_I & 0 & 0 & 0 & -(k_C+k_Q) & 0 & 0 & 0 & 0 & 0 & 0 \\
0 & 0 & 0 & k_{AB}^{(1)} & 0 & 0 & 0 & 0 & 0 & 0 & 0 & 0 & -k_I & k_C & 0 & 0 & 0 & 0 \\
0 & 0 & 0 & 0 & k_{AB}^{(1)} & 0 & 0 & 0 & 0 & 0 & 0 & 0 & 0 & -(k_C+k_I) & k_C & 0 & 0 & 0 \\
0 & 0 & 0 & 0 & 0 & k_{AB}^{(1)} & 0 & 0 & 0 & 0 & 0 & 0 & 0 & 0 & -k_C & 0 & 0 & 0 \\
0 & 0 & 0 & 0 & 0 & 0 & 0 & 0 & 0 & 0 & 0 & 0 & 0 & 0 & 0 & -k_{AB}^{(2)} & k_C & 0 \\
0 & 0 & 0 & 0 & 0 & 0 & 0 & 0 & 0 & 0 & 0 & 0 & 0 & k_I & 0 & 0 & 0 & -(k_C+k_{AB}^{(2)}) \\
0 & 0 & 0 & 0 & 0 & 0 & 0 & 0 & 0 & 0 & 0 & 0 & 0 & 0 & k_I & 0 & 0 & 0 & -(k_C+k_{AB}^{(2)})
\end{bmatrix}$$

$$\mathbf{X} = \begin{bmatrix}
C^{2+}PQ_AQ_B \\
C^{3+}PQ_AQ_B \\
C^{3+}P^+Q_AQ_B \\
C^{2+}PQ_A^-Q_B \\
C^{3+}PQ_A^-Q_B \\
C^{3+}P^+Q_A^-Q_B \\
C^{2+}PQ_AQ_BH_2 \\
C^{3+}PQ_AQ_BH_2 \\
C^{3+}P^+Q_AQ_BH_2 \\
C^{2+}PQ_A^-Q_BH_2 \\
C^{3+}PQ_A^-Q_BH_2 \\
C^{3+}P^+Q_A^-Q_BH_2 \\
C^{2+}PQ_AQ_B^- \\
C^{3+}PQ_AQ_B^- \\
C^{3+}P^+Q_AQ_B^- \\
C^{2+}PQ_A^-Q_B^- \\
C^{3+}PQ_A^-Q_B^- \\
C^{3+}P^+Q_A^-Q_B^-
\end{bmatrix}$$

quinone can be a much slower process (especially at alkaline pH range), determined primarily by the rate of the second electron transfer.

It is interesting to note that the model does not yield a strict linear relationship between reciprocal functions of rates of stationary cytochrome turnover and light reaction (k_{ct}^{-1} versus k_I^{-1}, Fig. 5). However, the deviation from the straight line in this representation is not very large. The value of vertical interception does not depend on light intensity and offers the inverse value of the maximum rate of cytochrome *c* photooxidation of the RC, which is characteristic of the internal thermal reactions, including donor/acceptor exchanges (k_{cyt} = 890 s^{-1} at pH 7.8). It can be seen that at light intensities as high as (expressed in terms of the photochemical rate constant) $k_I \approx 500\ s^{-1}$, commonly used for testing RCs with cytochrome turnover measurements, the turnover of the RC is about three times slower than the light-saturated value obtained from our analysis. Consequently, the illumination remained the major rate-limiting step in wild-type RCs, even at such high light intensities at neutral pH.

Rate-limiting steps in the photocycle

The cycling rate of the RC is determined by the slowest steps in the reaction path of Fig. 11. Light intensity, quinone and cytochrome exchange (availability), and (conformation coupled; Tiede et al., 1996) first and (proton coupled; Graige et al., 1996) second electron transfer can account for bottlenecks in the turnover. At moderate pH and under the usual light intensities, the intensity of the illumination is the rate-limiting step in cytochrome photooxidation. In this study, however, the rate of photochemistry could be made comparable to those of the thermal reactions of the RC. This opened the stage for the separation of rate-limiting steps in the turnover of the RC. The pH dependence of the rate of processes makes the distinction more straightforward (Fig. 10).

In the alkaline pH range (pH > 8), the rate of RC turnover decreased dramatically; as demonstrated in Fig. 6, the initial rapid cytochrome photooxidation was followed by relatively slow cytochrome turnover at high pH. Proton transfers and protonation-dependent electron transfer reactions can be made responsible for the decrease. Although the rate of the first electron transfer ($k_{AB}(1)$) decreases upon deprotonation of an acidic cluster centered around GluL212, it remains greater than $k_{AB}(2)$ (Fig. 10). It was recently observed that the apparent pK_a for the second proton was ~8.5 (McPherson et al., 1993, 1994); thus deceleration of the uptake of the second proton can be expected in this pH range. Our results indicate that neither $k_{AB}(1)$ nor the rate of the second proton transfer (included in k_Q in our model) is rate limiting, because the pH dependence of the rate of RC turnover is in full accordance with the drop in the second electron transfer rates, $k_{AB}(2)$, in the quinone acceptor system (Fig. 10). Thus the transfer of the first proton-coupled second electron from Q_A^- to Q_B^- is the rate-limiting step in the photocycle above pH 8 under high light excitation.

At near-neutral pH (6 < pH < 8), the highest turnover rates were observed. As the rates of all electron and proton transfer steps are larger than that of light excitation, the light intensity and the quinone exchange can be made responsible for the limitation of the cycling rate of the RC. The bottleneck at the quinone exchange could have been made more pronounced at higher light intensity, but even under our light excitation, a reasonable estimate could be made from the best fit of the model to the pH dependence of the observed cycling rate constants of the RC (Fig. 10). The rate of quinone exchange is slightly pH dependent, and a minimum value of $k_Q \approx 2.000\ s^{-1}$ can be determined at pH 6. Velthuys (1982) measured the turnover time of the Q_B site in photosystem II in the presence of inhibitors and concluded that Q_B was unbound in not more than 10 ms, which was similar to estimates for the uninhibited rate of transfer of electrons from QH_2 to the quinone pool. The estimate for the quinone exchange time in isolated bacterial RC was ~1 ms (Okamura and Feher, 1995).

The relatively large quinone exchange rate can be deduced from the set of quinone titration kinetics (Fig. 2). These observations indicated that, at neutral pH, the photostationary rate of cytochrome oxidation was not influenced by the size of the quinone pool. The rate of quinone exchange at the Q_B binding site of the RC remained comparable to the rate of photochemistry, even when the quinone pool was nearly exhausted.

The cytochrome titration experiments at neutral pH showed the opposite tendency (Fig. 3). The photostationary rate of cytochrome oxidation was significantly less at smaller than at larger cytochrome *c* concentration. The turnover was not limited by the light intensity, but by the cytochrome exchange at the cytochrome docking site of the RC. The exchange rate increased with cytochrome *c* concentration and, in the case of the largest cytochrome pool, could compete with that of the light reaction.

In the acidic pH range (pH < 6), the exchange of the cytochrome *c* will determine the cycling of the RC. Several crystallographic and binding studies, together with our low pH measurements, supported the electrostatic nature of forces that stabilize the cytochrome/RC complex (Tiede and Chang, 1988; Caffrey et al., 1992; Tiede at al., 1993; Meyer and Donohue, 1995). The dramatic changes in the rate of cytochrome *c* turnover were observed below pH 6 (Figs. 6–8 and 10), close to the reported isoelectric point (pI) of 6.1 for isolated RCs and far from 10.1, the pI for cytochrome *c* (Prince et al., 1974). The cytochrome exchange at the docking site of the RC consists of consecutive dissociation-association steps. Their rates are oppositely modified by changes in the electrostatics of the partners. It should be noted, however, that the rate of dissociation of the cytochrome/RC complex is significantly larger than that of association (Venturoli et al., 1990), and therefore the rate of association of the reduced cytochrome is the rate-limiting factor in the exchange process. The observed steep decrease

in the rate constant of the cytochrome exchange below pH 6 (Fig. 10) could be attributed to unfavorably changed electrostatic interaction between reduced cytochrome *c* and RC.

In contrast to mammalian cytochrome *c*, bacterial cytochrome c_2 has a much lower isoelectric point, mainly because of the presence of fewer lysine molecules (pI = 5.5; Bartsch, 1971). Its pI value is close to that of the RC, and therefore the two proteins have a similar overall charge at all pH values. That explains the observed pH-independent reaction rate between oxidized RC and reduced cytochrome c_2 (Prince et al., 1974). The use of cytochrome c_2 may prevent bacteria from decreasing the rate of turnover of the RC by cytochrome exchange under acidic conditions.

As demonstrated above, electrostatic interactions play a significant role in the determination of fast cytochrome exchange. Although the partners in the cytochrome/RC complex contain a complementary set of charged residues at the docking site, the contribution of individual charge pairs to the total interaction remains to be proved. The orientation of the bound cytochrome differs significantly in the models (Allen et al., 1988; Tiede and Chang, 1988; Caffrey et al., 1992; Tiede et al., 1993; Mathis, 1994), and binding of cytochrome and the rate of electron transfer of various members of the cytochrome family do not correlate directly with the magnitude of the charge difference at the docking domain (Meyer and Donohue, 1995). The electrostatics appears to only partly determine the function of the cytochrome/RC complex; other (e.g., hydrophobic and van der Waals) interactions are likely to contribute significantly to the cytochrome exchange (see, for similar systems, Hurley et al., 1996; Daff et al., 1996).

CONCLUSIONS

The mobile species of quinone and cytochrome from the pool are in stoichiometric and kinetic coupling to the primary quinone and dimer of the RC, exporting reducing and oxidizing equivalents from the RC during the photocycle, respectively. A minimal model with 18 redox states can account for the initial and stationary turnover of the RC. Despite the long isoprenoid chain and the densely packed Q_B region, the rate of quinone exchange is unexpectedly high and limits the turnover of the RC at near-neutral pH. Although the bound cytochrome *c* can rapidly donate flash-oxidized dimer, the overall process of exchange (mainly due to the unbinding of the oxidized cytochrome) can be much slower, and may limit the photocycle of the RC under stationary excitation. A quantitative comparison of the cycling rates of different RCs is worth making only if the same step is the bottleneck under otherwise identical conditions. In routine screening of mutants, care should be exercised, because light intensity and one of the electron or proton transfer steps are usually the rate-limiting processes in the turnover of wild-type and mutant RCs, respectively.

This work was supported by grants from the Hungarian Science Foundation (OTKA 17362/95), the Hungarian Ministry of Education (53205/96/XIV), Balaton (NP-715/95-F), and the International Human Frontier Science Program (RG-329/95 M).

REFERENCES

Allen, J. P., G. Feher, T. O. Yeates, H. Komiya, and D. C. Rees. 1988. Structure of the reaction center from *Rb. sphaeroides* R-26: protein-cofactor (quinones and Fe^{2+}) interactions. *Proc. Natl. Acad. Sci. USA.* 85:8487–8491.

Arlt, T., S. Schmidt, W. Kaiser, C. Lauterwasser, M. Meyer, H. Scheer, and W. Zinth. 1993. The accessory bacteriochlorophyll: a real electron carrier in primary photosynthesis. *Proc. Natl. Acad. Sci. USA.* 90: 11757–11761.

Arnoux, B., J. F. Gaucher, A. Ducruix, and F. Reiss-Husson. 1995. Structure of the photochemical reaction center of a spheroidene containing purple bacterium, *Rhodobacter sphaeroides* Y, at 3 Å resolution. *Acta Crystallogr.* D51:368–379.

Bartsch, R. G. 1971. Cytochromes: bacterial. *Methods Enzymol.* 23A: 344–363.

Caffrey, M. S., R. G. Bartsch, and M. A. Cusanovich. 1992. Study of cytochrome c_2 reaction center interaction by site-directed mutagenesis. *J. Biol. Chem.* 267:6317–6321.

Chang, C.-H., D. Tiede, J. Tang, U. Smith, J. Norris, and M. Schiffer. 1986. Structure of *Rb. sphaeroides* R-26 reaction center. *FEBS Lett.* 205: 82–86.

Clayton, R. K. 1980. Photosynthesis: Physical Mechanisms and Chemical Patterns. Cambridge University Press, Cambridge.

Cramer, W. A., and D. B. Knaff. 1990. Energy Transduction in Biological Membranes. Springer Verlag, New York.

Crofts, A. R., and C. A. Wraight. 1983. The electrochemical domain of photosynthesis. *Biochim. Biophys. Acta.* 726:149–185.

Daff, S., R. E. Sharp, D. M. Short, C. Bell, P. White, F. D. C. Mauson, G. A. Reid, and S. Chapman. 1996. Interaction of cytochrome *c* with flavocytochrome b_2. *Biochemistry.* 35:6351–6357.

Ermler, U., H. Michel, and M. Schiffer. 1994. Structure and function of the photosynthetic reaction center from *Rhobobacter sphaeroides. J. Bioenerg. Biomembr.* 26:5–15.

Feher, G., J. P. Allen, M. Y. Okamura, and D. C. Rees. 1989. Structure and function of bacterial photosynthetic reaction centers. *Nature.* 339: 111–116.

Graige, M. S., M. L. Paddock, J. M. Bruce, G. Feher, and M. Y. Okamura. 1996. Mechanism of proton-coupled electron transfer for quinone (Q_B) reduction in reaction centers of *Rb. Sphaeroides. J. Am. Chem. Soc.* 118:9005–9016.

Hurley, J. K., M. F. Fillat, C. G. Moreno, and G. Tollin. 1996. Electrostatic and hydrophobic interactions during complex formation and electron transfer in the ferredoxin-ferredoxin:$NADP^+$ reductase system from Anabaena. *J. Am. Chem. Soc.* 118:5526–5531.

Kleinfeld, D., M. Y. Okamura, and G. Feher. 1984. Electron transfer in reaction centers of *Rhodopseudomonas sphaeroides*. I. Determination of the charge recombination pathway of $D^+Q_AQ_B^-$ and free energy and kinetic relations between $Q_A^-Q_B$ and $Q_AQ_B^{2-}$. *Biochim. Biophys. Acta.* 766:126–140.

Kleinfeld, D., M. Y. Okamura, and G. Feher. 1985. Electron transfer in reaction centers of *Rhodopseudomonas sphaeroides*. II. Free energy and kinetic relations between the acceptor states $Q_A^-Q_B$ and $Q_AQ_B^{2-}$. *Biochim. Biophys. Acta.* 809:291–310.

Maróti, P. 1993. Flash-induced proton transfer in photosynthetic bacteria. *Photosynth. Res.* 37:1–17.

Maróti, P., D. K. Hanson, L. Baciou, M. Schiffer, and P. Sebban. 1994. Proton conduction within the reaction centers of *Rhodobacter capsulatus*: the electrostatic role of the protein. *Proc. Natl. Acad. Sci. USA.* 91:5617–5621.

Maróti, P., Sz. Osváth, Cs. Tápai, D. K. Hanson, and P. Sebban. 1995. From photons to protons in the photocycle of bacterial reaction center. *In* Photosynthesis: From Light to Biosphere, Vol. 1. P. Mathis, editor. Kluwer Academic Publishers, Norwell, MA. 419–424.

Maróti, P., Ch. Kirmaier, C. A. Wraight, D. Holten, and R. M. Pearlstein. 1985. Photochemistry and electron transfer in borohydride-treated photosynthetic reaction centers. *Biochim. Biophys. Acta.* 810:132–139.

Maróti, P., and C. A. Wraight. 1988. Flash-induced H^+ binding by bacterial photosynthetic reaction centers: comparison of spectrophotometric and conductometric methods. *Biochim. Biophys. Acta.* 934:314–328.

Mathis, P. 1994. Electron transfer between cytochrome c_2 and the isolated reaction center of the purple bacterium *Rhodobacter sphaeroides*. *Biochim. Biophys. Acta.* 1187:177–180.

McComb, J. C., R. R. Stein, and C. A. Wraight. 1990. Investigation on the influence of headgroup substitution and isoprene side-chain length in the function of primary and secondary quinones of bacterial reaction centers. *Biochim. Biophys. Acta.* 1015:156–171.

McPherson, P. H., M. Y. Okamura, and G. Feher. 1990. Electron transfer from the reaction center of *Rb. sphaeroides* to the quinone pool: doubly reduced Q_B leaves the reaction center. *Biochim. Biophys. Acta.* 1016: 289–292.

McPherson, P. H., M. Y. Okamura, and G. Feher. 1993. Light-induced proton uptake by photosynthetic reaction centers from *Rhodobacter sphaeroides* R-26.1. II. Protonation of the state $DQ_AQ_B^{2-}$. *Biochim. Biophys. Acta.* 1144:309–324.

McPherson, P. H., M. Schönfeld, M. L. Paddock, M. Y. Okamura, and G. Feher. 1994. Protonation and free energy changes associated with formation of Q_BH_2 in native and Glu-L212→Gln mutant reaction centers from *Rhodobacter sphaeroides*. *Biochemistry.* 33:1181–1193.

Meyer, T. E., and T. J. Donohue. 1995. Reaction center electron donors in anoxygenic photosynthetic bacteria. *In* Advances in Photosynthesis, Vol. 2, Anoxygenic Photosynthetic Bacteria. R. E. Blankenship, M. T. Madigan, and C. E. Bauer, editors. Kluwer Academic Publishers, Norwell, MA. 725–745.

Okamura, M. Y., R. J. Debus, D. Kleinfeld, and G. Feher. 1982. Quinone binding sites in reaction centers from photosynthetic bacteria. *In* Function of Quinones in Energy Conserving Systems. B. L. Trumpower, editor. Academic Press, San Diego, CA. 299–387.

Okamura, M. Y., and G. Feher. 1992. Proton transfer in reaction centers from photosynthetic bacteria. *Annu. Rev. Biochem.* 61:861–896.

Okamura, M. Y., and G. Feher. 1995. Proton-coupled electron transfer reactions of Q_B in reaction centers from photosynthetic bacteria. *In* Advances in Photosynthesis, Vol. 2, Anoxygenic Photosynthetic Bacteria. R. E. Blankenship, M. T. Madigan, and C. E. Bauer, editors. Kluwer Academic Publishers, Norwell, MA. 577–593.

Okamura, M. Y., R. A. Isaacson, and G. Feher. 1975. Primary acceptor in bacterial photosynthesis: obligatory role of ubiquinone in photoactive reaction centers of *Rhodopseudomonas sphaeroides*. *Proc. Natl. Acad. Sci. USA.* 72:3491–3495.

Osváth, Sz., G. Laczkó, P. Sebban, and P. Maróti. 1996. Electron transfer in reaction centers of *Rhodobacter sphaeroides* and *Rhodobacter capsulatus* monitored by fluorescence of the bacteriochlorophyll dimer. *Photosynth. Res.* 47:41–49.

Overfield, R. E., and C. A. Wraight. 1980. Oxydation of cytochromes *c* and c_2 by bacterial photosynthetic reaction centers in phospholipid vesicles. 1. Studies with neutral membranes. *Biochemistry.* 19:3322–3327.

Paddock, M. L., S. H. Rongey, E. C. Abresch, G. Feher, and M. Y. Okamura. 1988. Reaction centers from three herbicide-resistant mutants of *Rhodobacter sphaeroides* 2.4.1.: sequence analysis and preliminary characterization. *Photosynth. Res.* 17:75–96.

Paddock, M. L., S. H. Rongey, P. H. McPherson, A. Juth, G. Feher, and M. Y. Okamura. 1994. Pathway of proton transfer in bacterial reaction centers: role of aspartate-L213 in proton transfers associated with reduction of quinone to dihydroquinone. *Biochemistry.* 33:734–745.

Prince, R. C., R. J. Cogdell, and A. R. Crofts. 1974. The photo-oxidation of horse heart cytochrome *c*, and native cytochrome c_2 by reaction centers from *Rhodopseudomonas sphaeroides* R_{26}. *Biochim. Biophys. Acta.* 347:1–13.

Shinkarev, V. P. 1990. Function of Quinones in Bacterial Photosynthesis (in Russian). Viniti, Moscow.

Shinkarev, V. P., and C. A. Wraight. 1993. Electron and proton transfer in the acceptor quinone complex of reaction centers of phototrophic bacteria. *In* The Photosynthetic Reaction Center, Vol. 1. J. Deisenhofer and J. R. Norris, editors. Academic Press, San Diego, CA. 193–255.

Takahashi, E., P. Maróti, and C. A. Wraight. 1989. Site-directed mutagenesis of *Rhodobacter sphaeroides* reaction centers: the role of Tyr-L222. *In* Current Research in Photosynthesis. M. Baltscheffsky, editor. Kluwer Academic Publishers, Dordrecht. 169–172.

Takahashi, E., and C. A. Wraight. 1992. Proton and electron transfer in the acceptor quinone complex of *Rhodobacter sphaeroides* reaction centers: characterization of site-directed mutants of the two ionizable residues, Glu^{L212} and Asp^{L213}, in the Q_B binding site. *Biochemistry.* 31:855–866.

Takahashi, E., and C. A. Wraight. 1996. Potentiation of proton transfer function by electrostatic interactions in photosynthetic reaction centers from *Rhodobacter sphaeroides:* first results from site-directed mutation of the H subunit. *Proc. Natl. Acad. Sci. USA.* 93:2640–2645.

Tandori, J., L. Nagy, Á. Puskás, M. Droppa, G. Horváth, and P. Maróti. 1995. The Ile^{L229} → Met mutation impairs the quinone binding to the Q_B-pocket in reaction centers of *Rhodobacter sphaeroides*. *Photosyth. Res.* 45:125–146.

Taoka, S., H. H. Robinson, and A. R. Crofts. 1983. Kinetics of the reaction of the two electron gate of photosystem. II. Studies of the competition between plastoquinone and inhibitors. *In* The Oxygen Evolving System of Photosynthesis. Y. Inoue, A. R. Crofts, Govindjee, N. Murata, G. Renger, and K. Satoh. Academic Press, Tokyo. 369–381.

Tiede, D. M., and C. H. Chang. 1988. The cytochrome *c* binding surface of reaction centers from *Rhodobacter sphaeroides*. *Isr. J. Chem* 28: 183–191.

Tiede, D. M., A.-C. Vashishta, and M. R. Gunner. 1993. Electron-transfer kinetics and electrostatic properties of the *Rhodobacter sphaeroides* reaction center and soluble c-cytochromes. *Biochemistry.* 32: 4515–4531.

Tiede, D. M., J. Vazquez, J. Cordova, and P. A. Marone. 1996. Time-resolved electrochromism associated with the formation of quinone anions in the *Rhodobacter sphaeroides* R26 reaction center. *Biochemistry.* 35:10763–10775.

Van Gelder, B. F., and E. C. Slater. 1962. The extinction coefficient of cytochrome *c*. *Biochim. Biophys. Acta.* 58:593–595.

Van Rotterdam, B. J., W. Crielaard, H. V. Westerhoff, and K. J. Hellingwerf. 1995. Control over electron flow through the *Rhodobacter sphaeroides* reaction centre. *In* Photosynthesis: From light to Biosphere, Vol. I. Kluwer Academic Publishers, Dordrecht, The Netherlands. 707–710.

Velthuys, B. R. 1982. The function of plastoquinone in electron transfer. *In* Function of Quinones in Energy Conserving Systems. B. L. Trumpower, editor. Academic Press, San Diego. 401–408.

Venturoli, G., A. Mallardi, and P. Mathis. 1993. Electron transfer from cytochrome c_2 to the primary donor of *Rhodobacter sphaeroides* reaction centers. A temperature dependence study. *Biochemistry.* 32: 13245–13253.

Venturoli, G., B. A. Melandri, N. Gabellini, and D. Oesterhelt. 1990. Kinetics of photosynthetic electron transfer in artificial vesicles reconstituted with purified complexes from *Rhodobacter capsulatus*. I. The interaction of cytochrome c_2 with the reaction center. *Eur. J. Biochem.* 189:105–112.

Vermeglio, A., and R. K. Clayton. 1977. Kinetics of electron transfer between the primary and the secondary electron acceptor in reaction centers from *Rhodopseudomonas sphaeroides*. *Biochim. Biophys. Acta.* 461:159–165.

Wraight, C. A. 1979. Electron acceptors of bacterial photosynthetic reaction centers. II. H^+ binding coupled to secondary electron transfer in the quinone acceptor complex. *Biochim. Biophys. Acta.* 548:309–327.

Wraight, C. A. 1981. Oxidation-reduction physical chemistry of the acceptor quinone complex in bacterial photosynthetic reaction centers: evidence for a new model of herbicide activity. *Isr. J. Chem.* 21: 348–354.

Wraight, C. A., and R. K. Clayton. 1974. The absolute quantum efficiency of bacteriochlorophyll photooxidation in reaction centers. *Biochim. Biophys. Acta.* 333:246–260.

Wraight, C. A., and R. J. Shopes. 1989. Quinone binding and herbicide activity in the acceptor quinone complex of bacterial reaction centres. *In* Techniques and New Developments in Photosynthesis Research. J. Barber and R. Malkin, editors. Plenum Publishing Corporation, New York. 183–191.